



Effects of high temperature on the linear thermal expansion coefficient of Nanan granite

Zhennan Zhu^{1,3} · Shengqi Yang¹ · Ren Wang² · Hong Tian³ · Guosheng Jiang³ · Bin Dou³

Received: 3 August 2021 / Accepted: 11 January 2022 / Published online: 7 February 2022
© Akadémiai Kiadó 2022

Abstract

The evaluation of physico-mechanical characteristics of rocks after thermal treatment is a key issue in underground rock engineering projects such as exploitation of geothermal resources and geological disposal of nuclear waste. In this research, the lengths of cylindrical Nanan granite specimens were obtained before, during and after thermal treatment (up to 1000 °C) to investigate their linear thermal expansion coefficients, and the variation mechanisms were revealed by optical microscopic observations. According to the experimental results collected from the extensive corresponding literature, the relationships between the linear thermal expansion coefficients of various granites were also elaborated. The experimental results demonstrated that the linear thermal expansion coefficients of the granite in this study both under and after thermal treatment increase with temperature. Meanwhile, the linear thermal expansion coefficients increase rapidly above 500 °C, which is because of the quartz phase transition from α -phase to β -phase. The increase of linear thermal expansion coefficients of granite under and after thermal treatment closely relates to the thermal expansion of mineral crystals and the development and coalescence of intergranular and transgranular microcracks. The experimental results are expected to provide a reference to analytical calculations of thermophysical processes in granite.

Keywords High temperature · Granite · Thermal expansion coefficient · Microcracks · Quartz

✉ Ren Wang
137626257@qq.com

Zhennan Zhu
zhennanzhu0412@163.com

¹ State Key Laboratory for Geomechanics and Deep Underground Engineering, School of Mechanics and Civil Engineering, China University of Mining and Technology, Xuzhou 221116, China

² CNPC Engineering Technology R & D Company Limited, Beijing 102206, China

³ Faculty of Engineering, National Center for International Research on Deep Earth Drilling and Resource Development, China University of Geosciences, Wuhan 430074, China

1 Introduction

With economic development and population growth, more underground rock engineering projects involve high temperatures, such as exploitation of geothermal resources (Kumari et al. 2017; White et al. 2018), deep geological disposal of radioactive wastes (Abootalebi and Siemens 2018; Miao et al. 2021), underground tunnel fires (Wasantha et al. 2021), thermal effect in building stones (Ozguven and Ozcelik 2014; Vasanelli et al. 2021) and underground coal gasification (Wang et al. 2021a, b). The physico-mechanical characteristics of rock after thermal treatment are usually different from those at normal temperature. All of the above engineering applications are impacted by these variations. Therefore, the effect of thermal treatment on the physico-mechanical characteristics has become a popular topic of study in the field of rock mechanics.

In recent years, numerous laboratory tests have been carried out to study these effects. Studies of the physical properties of granite have shown that, with the increase of temperature, porosity, permeability and electronic conductivity increase, while bulk density, wave velocity and thermal conductivity degrade (David et al. 1999; Chaki et al. 2008; Yang et al. 2020). Studies on the mechanical characteristics of granite have focused on its strength and deformation characteristics. Generally, tensile strength (Roy et al. 2016; Zhao et al. 2018), compressive strength and elastic modulus (Shao et al. 2014; Fan et al. 2018; Zhang et al. 2018) deteriorate with temperature. With increasing temperature, a transformation for granite specimens from brittle characteristic to ductile plastic characteristic can be recognize from stress–strain curves because of the increase of microcrack density (Chen et al. 2012; Yang et al. 2017). Scanning electron microscopy (SEM) systems (Rathnaweera et al. 2018; Kumari et al. 2019), X-ray computed tomography (XCT) (Yang et al. 2017; Fan et al. 2018) and optical microscopy (Shao et al. 2014) are used to observe and discover the microscopic change mechanisms of the physico-mechanical characteristics of granite samples under/after thermal treatment.

Although the effects of thermal treatment on the physico-mechanical characteristics of granite specimens were comprehensively studied in the above reports, limited research is available on the effects of different temperatures on the linear expansion coefficient of granite specimens. Consequently, this work investigates the linear thermal expansion coefficients of granite specimens under/after thermal treatment over the range of 20 to 1000 °C, and the change mechanisms are revealed using optical microscope images of specimens after thermal treatment. The experimental data presented here are expected to support analytical calculations and numerical simulations (Tang et al. 2020) of thermos-physical processes in granites.

2 Experimental design

2.1 Specimen preparation

Granite used in this research is well-crystallized and reddish-brown, which was collected from Nanan county, Quanzhou city, China. According to ISRM (Franklin et al. 1979) suggested method, all specimens were cored from an intact block into cylinders with the height of 100 mm and diameter of 50 mm. The P-wave velocity and density of the specimens were 4167 ± 200 m/s and 2.596 ± 0.01 g/cm³, respectively. Based on the X-ray diffraction (XRD)

analysis results, the granite specimens were mainly composed of orthoclase (41.42%), plagioclase (30.79%), biotite (15.90%) and quartz (11.89%).

2.2 Experimental equipment and procedure

The granite samples were first placed in an oven for drying at 105 °C for 12 h to remove the effect of the original water (Meng et al. 2020). Next, the P-wave velocity, mass and size of the samples were measured using an ultrasonic concrete tester (RSM-SY5), an electronic balance and a Vernier caliper, respectively. More details about these experimental equipments can be found in our previous study (Zhu et al. 2021). The density was calculated through the weight and the volume (diameter and length) of the samples based on the methods recommended by ISRM (Franklin et al. 1979). After eliminating the specimens with an abnormal density or P-wave velocity, the left samples were separated into 6 groups, including a set of specimens without experiencing heating treatment. The temperature of wall rock in underground rock engineering may reach more than 1000 °C. For example, Ocampo et al. (2013) found out that the maximal temperature of upper rock layers can reach 1300 °C during coal gasification, and Gibb. (2000) pointed out that the temperature of the surrounding rock caused by the decomposition of radioactive nuclear wastes can even be up to 1500 °C. The maximum heating temperature of the furnace used in this study is 1100 °C. Therefore, the specimens were heated to the target test temperature (200, 400, 600, 800 and 1000 °C) using a muffle furnace (SG-XL1200). 5 °C/min was chosen as the heating rate to minimize thermal gradient in the heated specimens, since this heating rate might be a critical heating rate for reducing the effect of thermal gradient (or thermal shock) in granite (Chen et al. 2017; Wang et al. 2021a, b). In a recent study, 1 h has been verified to be enough for even heating in a rock specimen according to the results calculated by the numerical simulation (Wang et al. 2020). Therefore, the target temperatures of the heated samples were remained for 2 h in this study to avoid uneven heating of the interior of the specimens. When the constant temperature was over, the heated specimens were taken from the furnace, and the dimensions of each specimen were immediately measured under high-temperature condition by the Vernier caliper. We have tried our best to measure the dimensions of each specimen as quickly as possible to reduce the effect of heat loss of the specimens after exposure to air condition. Then, the granite samples were put back to the muffle furnace to cool naturally. Afterwards, the size and mass of each specimen were measured at normal temperature once again. Finally, the optical microscope was applied to observe the microstructural characteristics of granite exposed to different temperatures, and the experimental results are presented in Table 1.

3 Experimental results

3.1 Effects of temperature on linear thermal expansion coefficient

According to the definition of linear expansion coefficient, the thermal expansion coefficient under thermal treatment (α_u) and after thermal treatment (α_a) can be expressed as

$$\alpha_i = \frac{H_i - H_0}{H_0 \Delta t} \quad (1)$$

Table 1 Measured and calculated data for granite under and after various temperature treatments

Temp. (°C)	Number	$\rho_0(\text{g/cm}^3)$	$V_{p0}(\text{m/s})$	$H_0(\text{mm})$	$H_a(\text{mm})$	$H_s(\text{mm})$	$\alpha_a(10^{-6}/^\circ\text{C})$	$\alpha_s(10^{-6}/^\circ\text{C})$	$\rho_f(\text{mm/mm}^2)$	$W_a(\mu\text{m})$
20*	A-1	2.596	3333	100.87	100.87	100.87	0.00	0.00	0.17	6.61
	A-2	2.595	3226	100.38	100.38	100.38	0.00	0.00		
	A-3	2.597	3226	100.39	100.39	100.39	0.00	0.00		
200	B-1	2.595	3333	100.06	100.23	100.13	9.62	3.89	0.58	8.77
	B-2	2.598	3333	100.00	100.14	100.07	8.15	4.07		
	B-3	2.593	3226	100.52	100.67	100.60	8.11	4.24		
400	C-1	2.596	3226	99.95	100.53	100.22	15.27	6.93	1.02	16.93
	C-2	2.595	3226	100.02	100.50	100.22	12.54	5.26		
	C-3	2.593	3333	99.96	100.49	100.21	14.04	6.67		
500	D-1	2.591	3333	99.90	100.72	100.20	17.10	6.33	1.70	19.86
	D-2	2.597	3226	100.45	101.31	100.79	17.84	7.12		
	D-3	2.595	3226	100.91	101.66	101.32	15.55	8.53		
600	E-1	2.598	3333	100.48	101.94	101.13	24.94	11.15	1.95	25.16
	E-2	2.599	3333	100.91	102.26	101.51	23.07	10.37		
	E-3	2.595	3226	100.48	101.83	101.20	23.11	12.35		
800	F-1	2.598	3226	100.43	102.35	101.39	24.46	12.30	2.53	32.55
	F-2	2.596	3333	100.33	102.32	101.37	25.51	13.29		
	F-3	2.593	3226	100.44	102.33	101.55	24.08	14.13		
1000	G-1	2.596	3333	100.01	102.51	101.90	25.44	19.22	3.08	38.49
	G-2	2.598	3333	99.97	102.49	101.91	25.76	19.80		
	G-3	2.596	3333	100.52	102.92	102.41	24.29	19.19		

*' represents specimens without experiencing heating treatment

' ρ_0 ' is density of specimen not subjected to thermal treatment

' V_{p0} ' is longitudinal wave velocity of specimen without experiencing heating treatment

where $i = u$ or a ; H_0 , H_u and H_a are the average lengths of a specimen measured before, under and after thermal treatment; Δt is the change in temperature.

As Fig. 1 indicates, with the increase of temperature, the average values of α_u and α_a gradually increase, and the differences between the values of α_u and α_a is relatively larger between 500 and 600 °C than that below 500 °C. The values of α_u and α_a increase by 95.11 and 80.19% at 500 °C, respectively, compared to 200 °C, while they increase by 174.79% and 110.17% at 600 °C compared to 200 °C. At the same time, the average values of α_a after high temperature are always smaller than those values of α_u under in-situ high temperature.

However, the linear expansion coefficient under high temperature has scarcely changed when the temperature is heated to over 600 °C, which is mainly caused by the test method. When the specimen is taken from the furnace at above 600 °C, due to huge difference in temperature between heated specimens and air environment, the specimen will suffer a greater heat loss and cold contraction, which definitely has a great influence on the measurement of the linear expansion coefficient.

3.2 Effect of temperature on the microstructure

As Fig. 2 indicates, thin sections of specimens (enlarged 80 times) exposed to different temperatures were studied through the optical microscope. Microcrack density (ρ_f) is introduced to quantify the cracks in the rock specimens after high temperature (Fig. 2), which can be expressed as

$$\rho_f = \frac{L}{S} \quad (2)$$

where ρ_f is the microcrack density; L is the accumulative length of each microcrack; and S is total observed area in each sample.

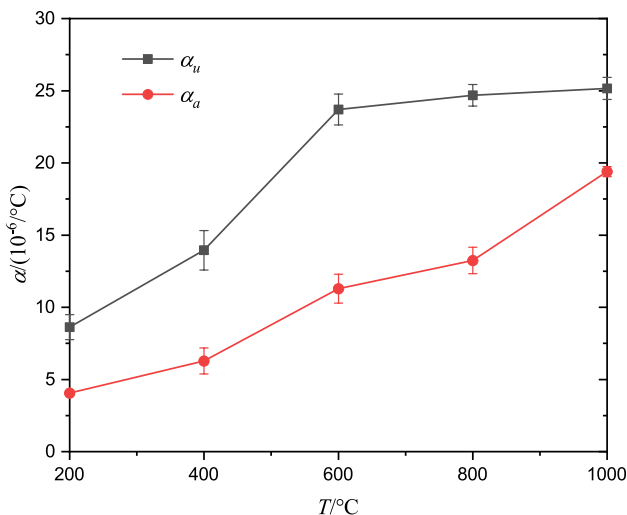


Fig. 1 Relationships between temperature and linear thermal expansion coefficients of granite

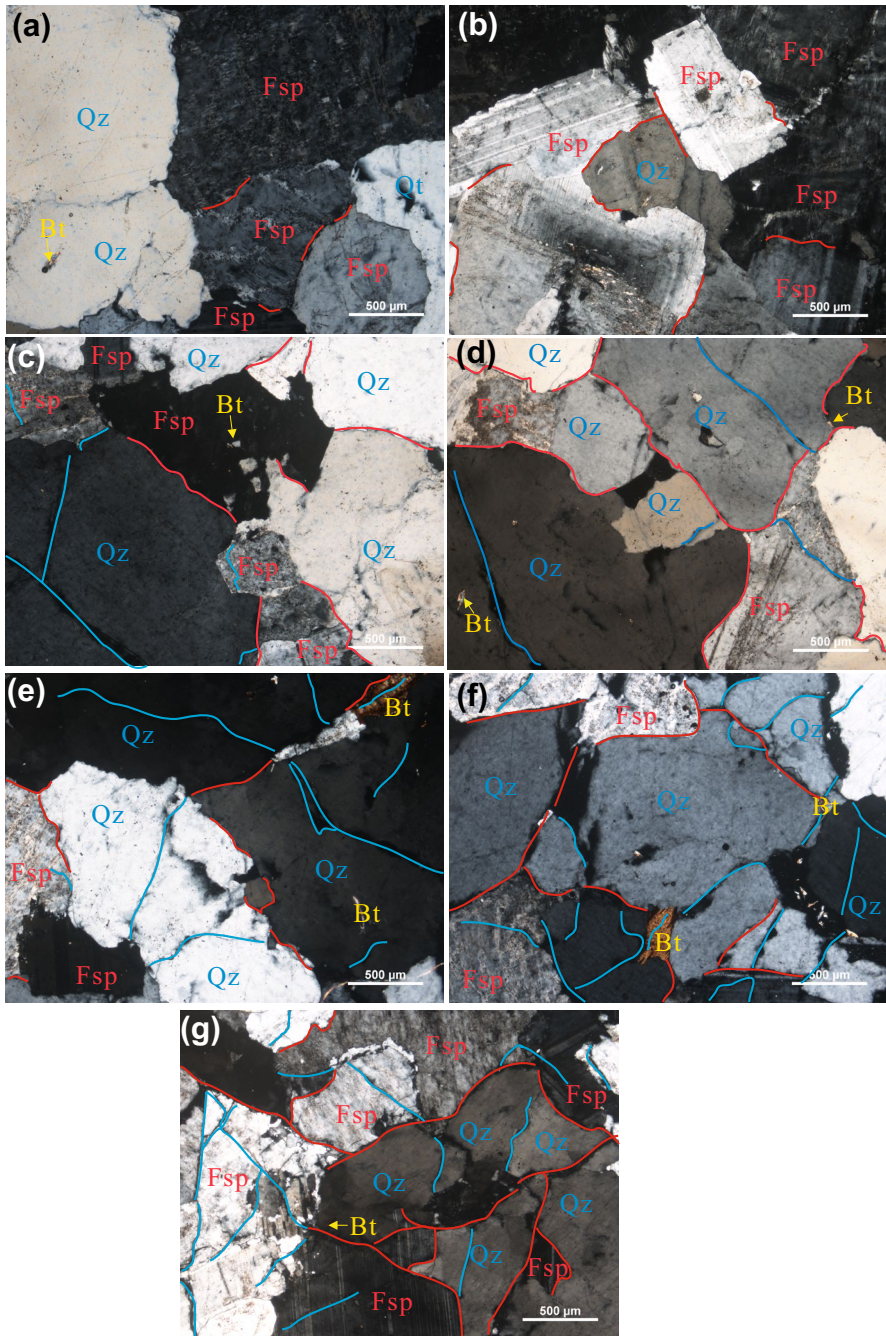


Fig. 2 Optical microscopic images of the specimens exposed to different temperatures (“Qz” stands for quartz; “Fsp” stands for feldspar; “Bt” is stands for biotite; blue lines represent “transgranular cracks”; red lines represent “intergranular cracks”)

In addition, the average width of microcracks was also calculated, and Table 1 and Fig. 3 present the details of microcracks (the average width and density). In the specimens without thermal treatment (Fig. 2a), the crystals are closely crystallized and very few intergranular microcracks are found, and the microcrack density is only 0.17 mm/mm^{-2} . At $200 \text{ }^\circ\text{C}$, the microcrack density begins to increase and reaches 0.55 mm/mm^{-2} . With the temperature increasing to $400 \text{ }^\circ\text{C}$, the density of microcrack grows to 1.02 mm/mm^{-2} and transgranular microcracks are found inside feldspar crystals (Fig. 2(c)), and the microcrack width changes greatly to $16.93 \text{ }\mu\text{m}$ from $6.61 \text{ }\mu\text{m}$ at normal temperature. At $600 \text{ }^\circ\text{C}$, many transgranular microcracks are found in quartz crystals (Fig. 2e), which is due to the phase transition of α -quartz to β -quartz at $573 \text{ }^\circ\text{C}$. Transgranular microcracks are also found inside biotite crystals. Therefore, the microcrack density and width both grow rapidly and reach 1.97 mm/mm^{-2} and $25.16 \text{ }\mu\text{m}$ from 1.70 mm/mm^{-2} to $19.86 \text{ }\mu\text{m}$ at $500 \text{ }^\circ\text{C}$. When the temperature further increases to $800 \text{ }^\circ\text{C}$, larger microdefects are observed, and the microcrack density and width further grow to 2.53 mm/mm^{-2} and $32.55 \text{ }\mu\text{m}$. Many microcracks in $1000 \text{ }^\circ\text{C}$ specimen widen further ($W_a = 38.49 \text{ }\mu\text{m}$), extend ($\rho_f = 3.08 \text{ mm/mm}^{-2}$) and coalesced. Finally, a crack network appears in the observed thin section in the granite specimen (Fig. 2g).

4 Discussion

The thermal expansion coefficient is a meaningful parameter of rock for underground engineering. Properties that have an influence on the thermal expansion of rock are mineral composition, porosity, properties of the fluid in pores and microcracks (Siegesmund et al. 2000). Of all these factors, thermal treatments do have a not negligible impact on the thermal expansion coefficient of rocks, especially in underground engineering. As Fig. 4 indicates, there are great variations of thermal-expansion behaviors between feldspar and quartz. The linear expansion coefficient of feldspar and quartz (the major mineralogical composition of granite) increase with high temperature, which induce the increase of linear

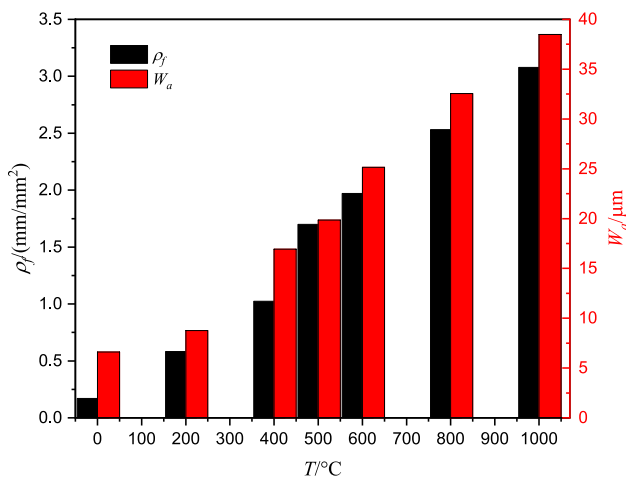


Fig. 3 Relations between microcrack density and width in observed thin section in specimens exposed to different temperatures

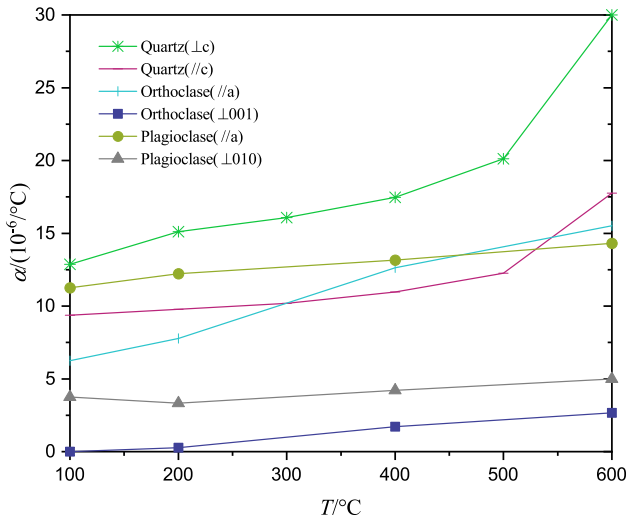


Fig. 4 Relationships between temperature and linear thermal expansion coefficients of granite main minerals (quoted from Somerton 1992)

expansion coefficients of granite under/after high-temperature treatment (Somerton 1992). Meanwhile, variations of expansion characteristics along various crystallographic axes of the same mineral (feldspar and quartz) are also presented in Fig. 4, where c, a, 001 and 010 are crystallographic axes of quartz and feldspar. For example, with the increasing temperature, the linear thermal expansion coefficient of quartz being perpendicular to c-axis is always larger than that being parallel to c-axis (Somerton 1992). As a result, these variations of expansion characteristics cause uneven expansion of mineral crystals upon heating and cause uneven deformation of granite minerals (Clark 1966). The uneven deformation induces thermal stress among granite minerals, and once the thermal stress concentration exceeds the yield strength of minerals, cracking begins to initiate (Yang et al. 2017). At the same time, the microcracks are widened and extended with the high temperature (Fig. 2). Thus, the increase of the linear thermal expansion coefficients of granite under and after thermal treatments is mainly caused by the thermal expansion of mineral crystals and the generation and development of numerous microcracks.

The linear thermal expansion coefficients of granite under in-situ high temperature are greater than these after thermal treatment (Fig. 1). This is because the minerals contract and some microcracks close again after cooling down. Permanent deformation causes the increase of the linear thermal expansion coefficients of granite after thermal treatment.

Based on a comprehensive review of international literature, the relationships between temperature and the thermal expansion coefficients of various granites are plotted in Fig. 5. The test parameters of thermal treatment and the mineral compositions of the granites are presented in Table 2. The table shows that the linear thermal expansion coefficients of various granites all increase with temperature to varying degrees. Above 500 °C, the linear thermal expansion coefficients abruptly increase. For example, the linear thermal expansion coefficients of BjG* and SdG increase by 62.14% and 114.04%, respectively. The linear thermal expansion coefficient of quartz also increases sharply between 500 and 600 °C, while the value of feldspar shows little change (Figs. 1 and 4), which corresponds to many transgranular microcracks being observed in quartz crystals at 600 °C (Fig. 2e). The

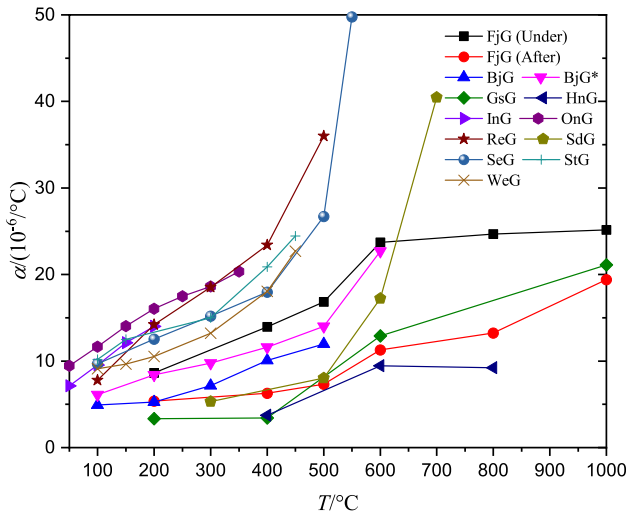


Fig. 5 Relationships between temperature and linear thermal expansion coefficients of various granites

behavior of quartz may be because the transition of α -quartz to β -quartz at atmospheric pressure occurs at 573 °C, causing a linear expansion of 0.45% (Somerton et al. 1992).

The relationship between temperature and the thermal expansion coefficient can be estimated using the equation:

$$\alpha_T = \alpha_0 \exp[b * (T - 20)] \quad (3)$$

where T represents temperature; α_T is linear expansion coefficient of rock under in-situ high temperature of T ; α_0 is the linear expansion coefficient of rock at normal temperature (20 °C); b is a constant determined by fitting experimental data.

The relationships between temperature and the thermal expansion coefficients of various granites are concluded in Table 2. The correlation coefficients of the thermal expansion coefficient after exposure to high temperatures are all above 0.871, which indicates that there are strong links between the linear expansion coefficient and temperature. Correlation coefficients of the linear expansion coefficient after high temperature show an exponential relation with temperature. However, the measurement of the linear expansion coefficient of granite above 600 °C is influenced by the test method, as a result, the correlation coefficient of the linear expansion coefficient under thermal treatment is only 0.768, which cannot reflect the real relations between temperature and the thermal expansion coefficient of granite under heating treatment. In the near future, we will try our best to improve the method and test equipment to find out more accurate changes of the thermal expansion coefficient of granite under heating treatment above 600 °C.

5 Conclusions

In this research, we investigate the linear thermal expansion coefficients of granite specimens during/after thermal treatment over the range of 20 to 1000 °C, and reveal the change mechanisms of linear thermal expansion coefficients of granite using optical microscope images. Based on an extensive review of the corresponding international literature, the

Table 2 Test parameters of thermal treatment and mineral compositions of studied granites

Abbr. ^a	Origin	Testing type ^b	N ^c	Sample Size ^d D×H	Sample shape	Mineral composition (%)				Empirical relations	Correlation Coefficient (R ²)	References
						Quartz	Feldspar	Biotite	Others			
FjG	Fujian China	Under & after	3	100×50	Cylinder	10.96	81.65	7.39	–	$\alpha_T = 10.27 \cdot \exp(0.00102 \cdot T/20)$ $(T/20) \leq \alpha_T = 6 \cdot \exp(0.017 \cdot T/20)$	0.768 0.972	This study
BjG	Beijing China	After	3	50×25	Cylinder	42	53	5	–	$\alpha_T = 3.51 \cdot \exp(0.00249 \cdot T/20)$	0.977	Tian et al. (2016)
BjG ^e	Beijing China	After	1	10×6×50	Cube	25	60	15	–	$\alpha_T = 3.48 \cdot \exp(0.00304 \cdot T/20)$	0.955	Li (2016)
GsG	Gansu China	After	3	100×50	Cylinder	21	70	5	4	$\alpha_T = 2.72 \cdot \exp(0.00208 \cdot T/20)$	0.906	Hu et al. (2016)
HnG	Henan China	After	5	100×50	Cylinder	–	–	–	–	–	–	Qiu and Lin (2006)
InG	India	After	1	25×6×6	Cube	39.5	58	1.5	1	$\alpha_T = 6.10 \cdot \exp(0.00428 \cdot T/20)$	0.978	Dwivedi et al. (2008)
OnG	Ontario Canada	After	–	65×32.5	Cylinder	–	–	–	–	$\alpha_T = 9.57 \cdot \exp(0.00225 \cdot T/20)$	0.955	Wai et al. (1982)
ReG	Remiremont France	After	–	–	–	27	65	5	3	$\alpha_T = 6.36 \cdot \exp(0.00343 \cdot T/20)$	0.983	Homand-Etienne (1989)
SdG	Shandong China	After	1	100×50	Cylinder	11.12	59.85	21.56	7.47	$\alpha_T = 1.43 \cdot \exp(0.00435 \cdot T/20)$	0.905	Yang et al. (2017)
SeG	Senones France	After	–	–	–	17	70	8	5	$\alpha_T = 3.55 \cdot \exp(0.00455 \cdot T/20)$	0.871	Homand-Etienne 1989
SiG	Stripa America	After	–	–	–	44	51	2	3	$\alpha_T = 9.24 \cdot \exp(0.00956 \cdot T/20)$	0.956	Heard and Page 1982
WeG	Westerly America	After	–	–	–	27	65	4	4	$\alpha_T = 6.15 \cdot \exp(0.00280 \cdot T/20)$	0.975	Heard and Page 1982

^a The abbreviations represent names of granites based on their origins

^b Tests were conducted on rock samples under/after thermal treatment

^c N represents the number of specimens in each group

^d D represents diameter and H represents length

relations between thermal expansion coefficient of granite after thermal treatment and temperature are drawn. The main conclusions can be briefly presented as follows:

1. The linear thermal expansion coefficients of Nanan granites after high temperature show an exponential relation with temperature; changes in the thermal expansion coefficients are more pronounced with increasing temperature. The values of α_u at 400, 500, 600, 800 and 1000 °C increase from those at 200 °C by 61.73%, 95.11%, 174.79%, 186.17 and 191.71%, respectively. The values of α_u at 400, 500, 600 and 800 °C are 121.9%, 129.7%, 109.9% and 86.5% larger than those of α_a .
2. The linear thermal expansion coefficients of granites rapidly increase above 500 °C, which is attributed to the quartz phase transition from the α -phase to β -phase. The increase in the linear expansion coefficient of granite under and after thermal treatment is closely related to thermal expansion of mineral crystals and the generation and development of microcracks.

Acknowledgements This work is jointly supported by the National Natural Science Foundation of China (No. 42077231, 41602374 and 41674180) and the National Key Research and Development Program of China (No. 2019YFB1504203).

Author contribution ZZN and TH designed the experiment, and WSF was a major contributor in writing the manuscript. YSQ analyzed and interpreted the experiment data. JGS and DB reviewed, edited and revised the manuscript. All authors read and approved the final manuscript.

Data availability All data generated or analysed during this study are included in this published article.

Declarations

Conflict of interest The authors declare that they have no conflicts of interest related to this work.

References

- Abootalebi P, Siemens G (2018) Thermal properties of engineered barriers for a Canadian deep geological repository. *Can Geotech J* 55(6):759–776
- Chaki S, Takarli M, Agbodjan WP (2008) Influence of thermal damage on physical properties of a granite rock: porosity, permeability and ultrasonic wave evolutions. *Constr Build Mater* 22(7):1456–1461
- Chen YL, Ni J, Shao W, Azzam R (2012) Experimental study on the influence of temperature on the mechanical properties of granite under uni-axial compression and fatigue loading. *Int J Rock Mech Min Sci* 56(15):62–66
- Chen S, Yang C, Wang G (2017) Evolution of thermal damage and permeability of Beishan granite. *Appl Therm Eng* 110:1533–1542
- Clark SP (1966) Handbook of physical constants. *Geol Soc Am* 97:459–482
- David C, Menéndez B, Darot M (1999) Influence of stress-induced and thermal cracking on physical properties and microstructure of La Peyratte granite. *Int J Rock Mech Min Sci* 36(4):433–448
- Dwivedi RD, Goel RK, Prasad VVR, Sinha A (2008) Thermo-mechanical properties of Indian and other granites. *Int J Rock Mech Min Sci* 45(3):303–315
- Fan LF, Gao JW, Wu ZJ, Yang SQ, Ma GW (2018) An investigation of thermal effects on micro-properties of granite by X-ray CT technique. *Appl Therm Eng* 140:505–519
- Franklin JA, Vogler UW, Szlavín J (1979) Suggested methods for determining water content, porosity, density, absorption and related properties and swelling and slake-durability index properties: part 1: suggested methods for determining water content, porosity, density, absorption and related properties. *Int J Rock Mech Mining Sci & Geomech Abstr* 16(2):143–151

- Gibb FG (2000) A new scheme for the very deep geological disposal of high-level radioactive waste. *J Geol Soc* 157:27–36
- Heard HC, Page L (1982) Elastic moduli, thermal expansion, and inferred permeability of two granites to 350 °C and 55 megapascals. *J Geophys Res Solid Earth* 87(B11):9340–9348
- Homand-Etienne F (1989) Heating effect on rock properties: thermal expansion and microcracking. In: D Fourmaintraux, V Maury (eds) *Rock at great depth 1*: 371–378, A. A. Balkema, Rotterdam, Germany.
- Hu SH, Zhang G, Zhang M, Jiang XL, Chen YF (2016) Deformation characteristics tests and damage mechanics analysis of Beishan granite after thermal treatment. *Rock Soil Mech* 37(12):3427–3436 (in Chinese)
- Kumari WGP, Ranjith PG, Perera MSA, Shao S, Chen BK, Lashin A, Al AN, Rathnaweera TD (2017) Mechanical behaviour of Australian strathbogie granite under in-situ stress and temperature conditions: an application to geothermal energy extraction. *Geothermics* 65:44–59
- Kumari WGP, Beaumont DM, Ranjith PG, Perera MSA, Avanthi Isaka BL, Khandelwal M (2019) An experimental study on tensile characteristics of granite rocks exposed to different high-temperature treatments. *Geomech Geophys Geo-Energy Geo-Resources* 6:47–64
- Li R (2016) Study on the thermal expansion characteristics of rock based on micromechanics. MS thesis, China University of Geosciences, Beijing, China
- Meng YY, Jing HW, Yin Q, Gu XW (2020) Investigation on mechanical and AE characteristics of yellow sandstone undergoing wetting-drying cycles. *KSCE J Civ Eng* 24:3267–3278
- Miao S, Pan PZ, Zhao XG, Shao CY, Yu PF (2021) Experimental study on damage and fracture characteristics of Beishan granite subjected to high-temperature treatment with DIC and AE techniques. *Rock Mech Rock Eng* 54:721–743
- Ocampo A, Arenas E, Chejne F, Espinel J, Londono C, Aguirre J, Perez J (2003) An experimental study on gasification of Colombian coal in fluidised bed. *Fuel* 82:161–164
- Ozguven A, Ozcelik Y (2014) Effects of high temperature on physico-mechanical properties of Turkish natural building stones. *Eng Geol* 183:127–136
- Qiu YP, Lin ZY (2006) Testing study on damage of granite samples after high temperature. *Rock Soil Mech* 27(6):1005–1010 (in Chinese)
- Rathnaweera TD, Ranjith PG, Gu X, Perera MSA, Kumari WGP, Wanniarachchi WAM, Haque A, Li JC (2018) Experimental investigation of thermomechanical behaviour of clay-rich sandstone at extreme temperatures followed by cooling treatments. *J Rock Mech Min Sci* 107:208–223
- Roy DG, Singh TN (2016) Effect of heat treatment and layer orientation on the tensile strength of a crystalline rock under Brazilian test condition. *Rock Mech Rock Eng* 49(5):1–15
- Shao SS, Wasantha PLP, Ranjith PG, Chen BK (2014) Effect of cooling rate on the mechanical behavior of heated Strathbogie granite with different grain sizes. *J Rock Mech Min Sci* 70:381–387
- Siegesmund S, Ullemeyer K, Weiss T, Tschegg EK (2000) Physical weathering of marbles caused by anisotropic thermal expansion. *Int J Earth Sci* 89(1):170–182
- Somerton WH (1992) Thermal properties and temperature-related behavior of rock/fluid systems. Elsevier, Amsterdam, pp 22–29
- Tang YJ, Ma TS, Chen P, Ranjith PG (2020) An analytical model for heat extraction through multi-link fractures of the enhanced geothermal system. *Geomech Geophys Geo-Energy Geo-Resources* 2020:6
- Tian H, Mei G, Zheng MY (2016) The physical and mechanical properties of rocks after high temperature. China university of Geosciences Press, Wuhan, pp 48–59
- Vasanelli E, Quarta G, Micelli F, Calia A (2021) The effects of an historical fire on a porous calcarenite from an industrial-archaeological building in the south of Italy. *Eng Geol* 292:106270
- Wai RSC, Lo KY, Rowe RK (1982) Thermal stress analysis in rocks with nonlinear properties. *J Rock Mech Min Sci* 19(5):211–220
- Wang F, Konietzky H, Frühwirth T, Li YW, Dai YJ (2020) The influence of temperature and high-speed heating on tensile strength of granite and the application of digital image correlation on tensile failure processes. *Rock Mech Rock Eng* 53:1935–1952
- Wang JT, Zuo JP, Sun YJ, Wen JH (2021a) The effects of thermal treatments on the fatigue crack growth of Beishan granite: an in situ observation study. *Bull Eng Geol Env* 80:1541–1555
- Wang SF, Sun Q, Wang QN, Luo T, Zhang H (2021) Responses of the magnetic susceptibility and chromaticity of loess to temperature in a coal fire area. *Acta Geod et Geophys*. <https://doi.org/10.1007/s40328-021-00349-1>
- Wasantha PLP, Guerrieri M, Xu T (2021) Effects of tunnel fires on the mechanical behaviour of rocks in the vicinity—a review. *Tunn Undergr Space Technol* 108:103667

- White M, Fu PC, McClure M, Danko G, Elsworth D, Sonnenthal E, Kelkar S, Podgorney R (2018) A suite of benchmark and challenge problems for enhanced geothermal systems. *Geomech Geophys Geo-Energy Geo-Resources* 4:79–117
- Yang SQ, Ranjith PG, Jing HW, Ju Y (2017) An experimental investigation on thermal damage and failure mechanical behavior of granite after exposure to different high temperature treatments. *Geothermics* 65:180–197
- Yang L, Sun Q, Hu JJ, Li CB (2020) Effects of temperature and pressure on electrical conductivity and wave velocity of basalt: a review. *Acta Geod Geoph* 56(3):177–191
- Zhang F, Zhao JJ, Hu DW, Skoczylas F, Shao JF (2018) Laboratory Investigation on physical and mechanical properties of granite after heating and water-cooling treatment. *Rock Mech Rock Eng* 51(3):677–694
- Zhao Z, Liu Z, Pu H, Li X (2018) Effect of thermal treatment on Brazilian tensile strength of granites with different grain size distributions. *Rock Mech Rock Eng* 51(4):1293–1303
- Zhu ZN, Tian H, Mei G, Jiang GS, Dou B, Xiao P (2021) Experimental investigation on mechanical behaviors of Nanan granite after thermal treatment under conventional triaxial compression. *Environ Earth Sci* 80(2):46